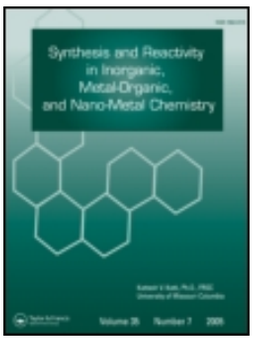

Taylor & Francis
Taylor & Francis Group

Synthesis and Reactivity in Inorganic, Metal-Organic, and Nano-Metal Chemistry

ISSN: 1553-3174 (Print) 1553-3182 (Online) Journal homepage: https://www.tandfonline.com/loi/lsrt20

Synthesis and Characterization of Polyhydroxybutyrate Coated Magnetic Nanoparticles: Toxicity Analyses on Different Cell Lines

Serap Yalcin, Rouhollah Khodadust, Gozde Unsoy, Immihan Ceren Garip, Zahide Didem Mumcuoglu & Ufuk Gunduz

To cite this article: Serap Yalcin, Rouhollah Khodadust, Gozde Unsoy, Immihan Ceren Garip, Zahide Didem Mumcuoglu & Ufuk Gunduz (2015) Synthesis and Characterization of Polyhydroxybutyrate Coated Magnetic Nanoparticles: Toxicity Analyses on Different Cell Lines, Synthesis and Reactivity in Inorganic, Metal-Organic, and Nano-Metal Chemistry, 45:5, 700-708, DOI: 10.1080/15533174.2013.831448

To link to this article: https://doi.org/10.1080/15533174.2013.831448

Synthesis and Reactivity in Inorganic, Metal-Organic, and Nano-Metal Chemistry (2015) 45, 700–708

ISSN: 1553-3174 print / 1553-3182 online
DOI: 10.1080/15533174.2013.831448

Taylor & Francis
Taylor & Francis Group

Synthesis and Characterization of Polyhydroxybutyrate Coated Magnetic Nanoparticles: Toxicity Analyses on Different Cell Lines

SERAP YALCIN[1], ROUHOLLAH KHODADUST[2], GOZDE UNSOY[2], IMMIHAN CEREN GARIP[3], ZAHIDE DIDEM MUMCUOGLU[3] and UFUK GUNDUZ[2]

[1]*Department of Food Engineering, Ahi Evran University, Kirsehir, Turkey*
[2]*Department of Biotechnology, Middle East Technical University, Ankara, Turkey*
[3]*Department of Molecular Biology and Genetics, Middle East Technical University, Ankara, Turkey*

Received 9 May 2013; accepted 27 July 2013

In this study, polyhydroxybutyrate (PHB) coated magnetic nanoparticles were prepared which are targetable to tumor cells in the presence of a magnetic field. The structural properties, functional groups, size distribution, and magnetic properties of the synthesized PHB coated magnetic nanoparticles were characterized by X-ray diffraction, Fourier transform infrared spectrometer, transmission electron microscopy, dynamic light scattering, vibrating sample magnetometry, and thermogravimetric analysis. PHB coated nanoparticles are efficiently internalized by the cancer cells in culture, without cytotoxicity. The results demonstrated that PHB coated iron oxide nanoparticles are suitable for targeted delivery of drugs such as chemotherapeutics, siRNA, miRNA, or antibodies.

Keywords: polyhydroxybutyrate, magnetic nanoparticle, anticancer agents, cytotoxicity, genotoxicity

Introduction

Magnetic nanoparticles (MNPs) are potential theranostic agents having a wide range of applications including magnetic resonance imaging (MRI) and therapy. Surface functionalized and targeted MNPs are focus of interest in diagnostics studies because they can be used for detection of variety of diseases such as cardiovascular disease,[1] neurological disease,[2] and cancer.[3] Besides being contrast agents in MRI, MNPs can deliver therapeutics that can be monitored at the same time. These properties of MNPs pave the way for diagnosis of tumors, chemotherapeutic monitoring, and simultaneous prognosis of treatment.[4,5]

The core material of MNPs can be magnetite (Fe_3O_4) or maghemite (γ-Fe_2O_3). Although magnetite is favored due to its superior magnetic characteristics, maghemite is more suitable for biomedical applications. Toxicity of MNPs is controversial but it is implicated that maghemite is less likely to cause any health hazard because iron(III) ions are already present in human body without creating any adverse effect.[6–9] MNPs are advantageous in drug delivery application, as they can be targeted with an applied magnetic field gradient. Especially in cancer treatment targeted delivery approach is substantial, as chemotherapeutic agents are circulated throughout the body causing toxicity to healthy tissues. Hence, the MNP delivery system will decrease the toxicity and nonselectivity of anticancer drugs.[10] This system will also increase the drug efficiency and circulation time. Also *in vivo* studies in rats indicate that MNPs did not affect liver enzyme levels in long term and also did not cause any induction of oxidative stress, thus they can be safely used.[11–13]

Following the administration, stable maintenance of nanoparticles in circulation depends on the quality of surface, hydrophobicity, and size of the material. Due to their surface hydrophobicity, iron oxide nanoparticles are subjected to opsonization, which causes recognition of nanoparticles by reticuloendothelial system and their clearance from the body.[7] Also magnetite nanoparticles are usually negatively charged if synthesized through the coprecipitation of Fe^{2+} and Fe^{3+} in ammonia or NaOH solution[14] and it results in agglomeration. In order to improve the *in vivo* circulation time of nanoparticles, prevent agglomeration, and make them soluble in bloodstream mostly, polymer coating is preferred. Importantly coating material should not affect the magnetic behavior of the nanoparticle dramatically and should balance the magnetic and Van der Waals forces acting on the nanoparticle by creating repulsive forces.[15] There are many different synthetic and natural polymers used for

Address correspondence to Serap Yalcin, Ahi Evran University, Faculty of Engineering–Architecture, Department of Food Engineering, 40000, Kirsehir, Turkey. E-mail: syalcin@ahievran.edu.tr
Color versions of one or more of the figures in the article can be found online at www.tandfonline.com/lsrt.

coating of nanoparticles such as dextran, poly(aniline), poly (ethyleneglycol), and polyesters such as poly(lactic acid) and poly(hydroxybutyrate).[8] In this study poly(hydroxybutyrate) (PHB), which belongs to the poly(hydroxyalkanoate) (PHA) family is used as a coating polymer. PHAs are linear biodegradable polyesters naturally synthesized by bacteria as a storage polymer. They are also synthesized for large-scale usage by biotechnological methods. PHAs can be produced by many different bacterial strains./16] There are many types of PHAs such as PHB (poly-3-hydroxybutyrate), PHV (poly-3-hydroxyvalerate), and PHHx (poly-3-hydroxyhexanoate), among which PHB is widespread.[12] They are of great interest for researchers in different disciplines including medicine, biotechnology, agriculture, and industry.[17] PHB is biodegradable and known that they can be degraded either nonenzymatically or enzymatically by PHA hydrolases and PHA depolymerases.[16,18] Further studies implied no toxic effect of PHB during *in vivo* applications.[19] The product of degradation, D-3-hydroxy butyrate is normally present in the human blood at concentrations of 1.3 mmol L^{-1}.[20,21] In biological environments they are degraded to end products of CO_2 and H_2O and the rate of their degradation is low.[22] PHB degradation rate both *in vivo* and *in vitro* depends on several parameters. When PHB is a copolymer (i.e., polyhydroxybutyrate-3-co-valerate) degradation rate may decrease.[23,24]

In this study, we developed a new method that enabled for the first time *in situ* and PHB coated MNPs, involving the coprecipitation of iron salts in the presence of PHB. The structural properties, functional groups, size distribution and magnetic properties of the synthesized nanoparticles were characterized by XRD, TGA, FT-IR, TEM, VSM, and DLS analyses. The synthesized nanoparticles may be used for medical applications such as targeted drug delivery, without cytotoxicity and genotoxicity.

Experimental

Reagent and Instruments

Iron(II) chloride tetrahydride (FeCl2.4H2O) and iron(III) chloride hexahydrate (FeCl3.6H2O) were obtained from Merck Germany; PHB and ammonium hydroxide (NH4OH), FITC (fluorescein isothiocyanate), RPMI-1640, FBS, Trypsin–EDTA, PBS (phosphate buffered saline), and gentamicin were purchased from Sigma-Aldrich Chemie GmbH, Germany. XTT cell proliferation assay kit (XTT) was supplied by Biological Industries, Israel Beit Haemek LTD. The equipment information: TEM: FEI/Tecnai G2 F30; DLS: Malvern/Nano ZS; Microscope: Olymphus/CKX41, VSM: Cryogenic Limited PPMS. VSM: ADE Magnetics EV/9 Vibrating Sample Magnetometer (VSM), Max applied field: 30000 Oe, sensitivity: 10–6 emu.

Synthesis of Magnetic Iron Oxide Nanoparticles

Magnetic iron oxide (Fe_3O_4) nanoparticles were synthesized for comparison purpose by the co-precipitation of Fe(II) and Fe(III) salts at 1:2 ratio in 150 mL deionized water within a five-necked glass balloon. The glass balloon is placed on a heating mantle and stirred by a glass rod of mechanical stirrer, which is inserted into the middle neck of the balloon. It is stirred vigorously in the presence of nitrogen (N_2) gas at 90°C. The nitrogen gas prevents oxidation. Ammonium hydroxide (NH_4OH) is added to the system dropwise. The process ends by washing with deionized H_2O until the solution pH is 9.0.

In Situ *Synthesis of PHB Coated Magnetic Iron Oxide Nanoparticles*

PHB coated magnetic iron oxide nanoparticles were *in situ* synthesized by the coprecipitation of Fe(II) and Fe(III) salts in the presence of PHB molecules with some modifications of Xiong et al.[25]

Iron salts (1.34 g of $FeCl_2$ $4H_2O$ and 3.40 g of $FeCl_3$ $6H_2O$) were dissolved in 30 mL of 1% PHB solution. Under the nitrogen (N_2) gas flow and by vigorously stirring at 2500 rpm. The ammonia solution (32%, NH_4OH) was added very slowly to produce smaller sized nanoparticles. The resulting solution was stirred for an additional 2–3 h. The colloidal PHB coated magnetic Fe_3O_4 nanoparticles were extensively washed with ethanol and separated by magnetic decantation for several times. The PHB coated and uncoated magnetic Fe_3O_4 nanoparticles were separated by magnetic decantation for several times.

Characterization of Bare and PHB Coated MNPs

Crystal structures of synthesized MNPs were analyzed by XRD. The chemical groups and chemical interactions involved in synthesized MNPs were identified using the FTIR methods. The sizes of magnetic core and morphological properties were observed through TEM images. The hydrodynamic sizes were determined with DLS measurements. The qualitative and quantitative information about the volatile compounds of the nanoparticles have been provided by TGA. Magnetic materials showing a superparamagnetic behavior have zero value of remanence and coercivity. The remanence and coercivity observed in the hysteresis loops of Fe_3O_4 and PHB coated Fe_3O_4 nanoparticles were measured at 37°C. Magnetic properties of MNPs and magnetic hysteresis curve were determined through VSM analyses. Three replicates were measured for each analysis including synthesis of MNPs and the results were averaged with standard deviation.

Cellular Internalization of FITC Binding PHB Coated Nanoparticles

PHB coated iron oxide nanoparticles were incubated with breast cancer (MCF-7, SKBR-3) cell lines in six-well plates and their photographs (scattering light microscope) were taken with time intervals during the incubation to determine their cellular internalization. In addition, PHB-MNPs were conjugated with fluorescent FITC, which was

applied onto breast cancer (MCF-7) cell lines. The resultant FITC-conjugated MNPs were visualized by confocal microscopy.

Cytotoxicity of PHB Coated Nanoparticles

MCF-7, SKBR-3, and HeLa human breast and ovarian cancer cells were used for the cell studies. Cells were grown in 75T culture flasks in RPMI/1640 culture medium supplemented with 10% FBS, and 1% gentamicin solution at 37°C under 5% CO_2. The cells were subcultured 2–3 times per week with 0.25% trypsin–EDTA. Antiproliferative effects of PHB coated nanoparticles on cells were evaluated by means of the Cell Proliferation Kit (Biological Industries) according to manufacturer's instructions. Assay was a colorimetric test based on the reduction tetrazolium salt, XTT to colored formazan products by mitochondria of live cells. In brief, cells were seeded to 96-well microtiter plates (Greiner) at a concentration of 5.0×10^4 cells/well and incubated for 72 h in medium containing horizontal dilutions of nanoparticles. In each plate assay was performed with a column of blank medium control and a cell control column. Then, XTT reagent was added and soluble product was measured at 500 nm with Spectromax 340, 96-well plate reader (Molecular Devices, USA).

Genotoxicity of PHB Coated MNPs

The comet assay (single-cell gel electrophoresis technique [SCGE]), is a simple, sensitive, fast, and effective method, even for extremely small samples of cells, and applicable to cells from any organ of eukaryotic organisms. This assay can be used to estimate DNA damage at the individual cell level through DNA single and double-strand breaks, DNA-DNA/DNA-protein cross-links, oxidatively induced base damages, alkali-labile sites, and open repair sites.[26,27] To investigate the DNA damage induced by PHB coated MNPs in human breast and ovarian cancer cells, we determined the comet assay as described by Singh et al.[26] MCF-7, SKBR-3, and HeLa cells were added to a six-well plate and the culture was maintained at 37°C in a 5% CO_2 atmosphere. After 24 h of incubation, the cells were exposed to PHB coated MNPs for 24 h. The cells were trypsinized and cell suspension was mixed with 0.5% low melting point agarose and added to the slides, which were immediately covered with coverslips. After removing the cover-glass, all slides were immersed for 1 h at 4°C in a lysing solution (2.5 M NaCl, 100 mM EDTA, 10 mM Tris, NaOH to pH 10, to which 1% Triton X-100, 1% N-lauryl sarcosine, and 10% DMSO were freshly added) in the dark. After lysis, the slides were washed with PBS. The slides were placed in an electrophoresis tank containing freshly prepared alkaline buffer (300 mM NaOH, 1m M EDTA, pH > 13), and the electrophoresis was conducted at room temperature during 20 min at 300 mA and 25 V. After the stage of electrophoresis, the slides were taken from the tank and washed for three times during 5 min with neutralizing buffer (0.4 M Tris, pH: 7.5) and washed three times with PBS. Then cells stained with ethidium bromide solutions (2 μg/mL). The slides were dried and then observed using the fluorescence microscope (Olympus BX50).

Results and Discussion

In the synthesis of MNPs, the conditions have been optimized by adjusting the temperature (20–90°C). Crystal structures were formed at the temperatures above 50°C. Pure Fe_3O_4 was obtained at 90°C. The characteristic properties of synthesized bare and PHB coated MNPs have been analyzed by various methods.

XRD

The crystal structure of synthesized iron oxide (Fe_3O_4) nanoparticles was determined by XRD. Diffraction peaks observed are characteristic peaks of the magnetite (Fe_3O_4) crystal having an inverse cubic spinel structure by comparison with standards in Figure 1. XRD results revealed the presence of the Fe_3O_4 crystals in the synthesized nanoparticles bare or PHB coated. Even the peak positions were unchanged, which illustrated that the PHB binding process did not result in the phase change of Fe_3O_4. No evidence of impurities was found in the XRD pattern. The peaks shown in the XRD pattern of the prepared sample are sharp and intense, indicating crystallinity of the sample. The particle sizes can be quantitatively evaluated from the XRD data using the Scherrer equation, which gives a relationship

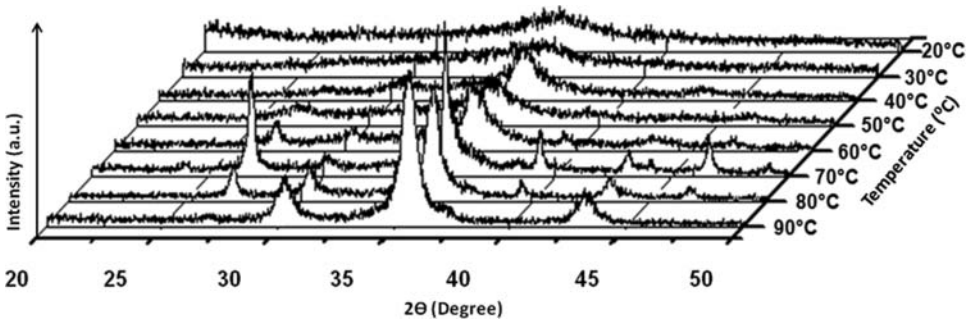

Fig. 1. X-ray powder diffraction (XRD) patterns of synthesized iron oxide (Fe_3O_4) nanoparticles in different temperatures.

between peak broadening in XRD and particle size.

$$D = k\lambda/(\beta \cdot cos\theta)$$

where k is Scherrer constant (0.89), λ the X-ray wavelength (nm), β the peak width of half-maximum, and θ the Bragg diffraction angle.[14]

FTIR

In order to confirm the chemical composition of synthesized nanoparticles, FTIR spectra were obtained. The peak located in the 583 cm^{-1} region, characteristic for the Fe-O group, is found in bare and PHB coated nanoparticles spectra, confirming that the products contain magnetite. All characteristic peaks of PHB and iron oxide were present in the spectrum of PHB-MNP and Table 1.[28] FTIR results showed the presence of magnetite in nanoparticle. Also the FTIR study showed the presence of PHB in this structure of magnetic nanoparticle. A strong peak at 1728 cm^{-1} indicates the presence of PHB. Also the other peaks obtained at 1285 cm^{-1} and 1181 cm^{-1} are much closer to the identified peaks for PHB (Figure 2).

Table 1 Characteristic FTIR bands of PHB polymer

Band assignment	Wavenumber (cm^{-1})
C-H stretching vib.	3020–2987
CH_3 antisym. stretching	2982–2956
CH_2 antisym. stretching	2952–2899
CH_3 sym. stretching	2892–2850
C=O (amorphous)	1775–1727
C=O (crystalline)	1729–1698
CH_3 antisym. stretching	1485–1425
CH_3 sym. deformation	1401–1368
CH def./CH_3 sym. deformation	1383–1341
CH deformation	1333–1248
C-O-C stretching	1246–1212
C-O-C stretching	1213–1158
CH_3 rocking	1160–1115
C-O-C	1115–1084
C-O stretching	1085–1020

TEM Analyses of PHB Coated MNPs

Size and morphology of synthesized MNPs and PHB coated MNPs have been observed by TEM. Obtained images showed that (Figures 3a and 3b) the synthesized PHB-MNPs are almost spherical and have more uniform size distribution as compared to bare MNPs. The average diameters are around 18–20 nm (bare MNP) and 30–35 nm (PHB-MNPs). Sizes of the nanoparticles were determined with TEM studies, and were found as 30–35 nm. Results of TEM showed that nanoparticles have smooth surface and uniform size distribution (about 30–35 nm for coated nanoparticles and 18 nm for bare nanoparticles). The particles sizes below 1 μm can be administrated intravenously, subcutaneously and intramuscularly.[29] MNPs coated with PHB are about 30–35 nm so their administration *in vivo* will not probably result in any damage to tissues or blood vessels, since the smallest blood capillary diameter is for 4 μm.[30]

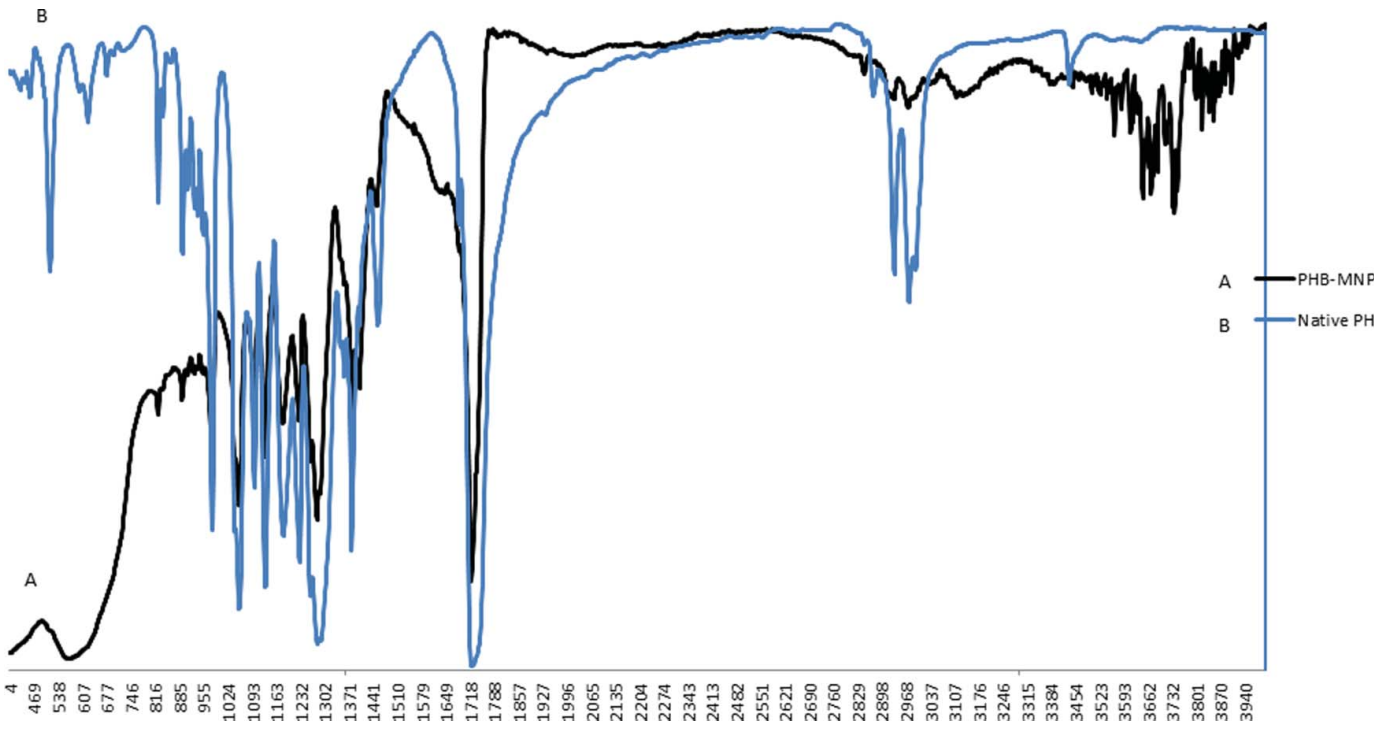

Fig. 2. Fourier-transform infrared spectra (FT-IR) of PHB coated iron oxide nanoparticle and native PHB.

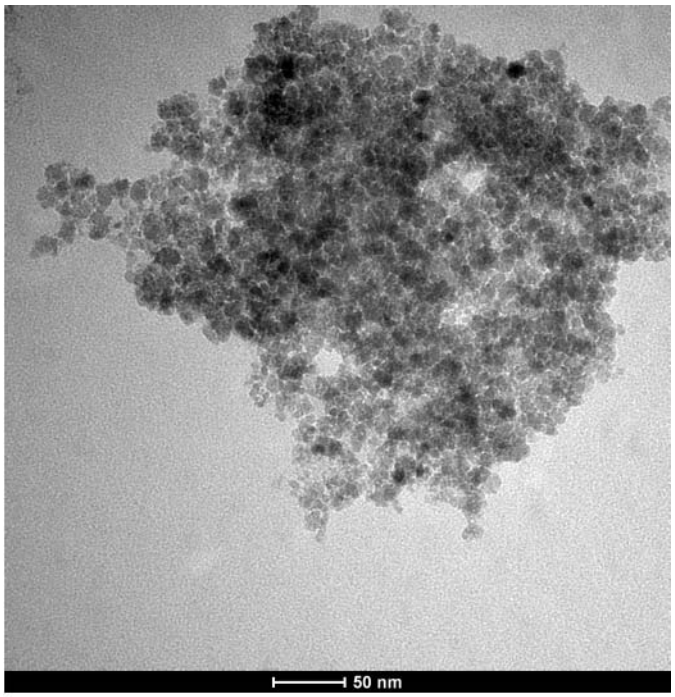

(A)

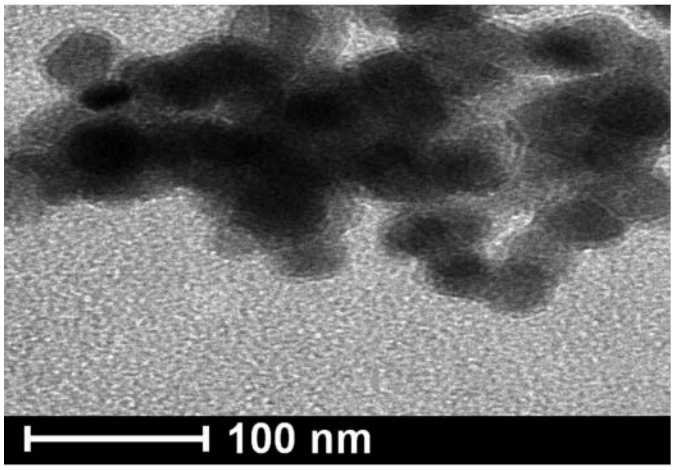

(B)

Fig. 3. (a) TEM images of Fe_3O_4 nanoparticles. **(b)** TEM images PHB-MNPs nanoparticles (size between 30 and 35 nm).

DLS

DLS is concerned with measurement of particles suspended within a liquid. The average sizes of PHB coated MNPs were found as 100 nm PHB-MNPs in DLS measurements (data not shown). There was not uncoating nanoparticles by DLS measurements. Average size of the PHB coated MNPs is about 100 nm and the intensity of 99.9% by DLS analysis.

The results are in parallel with the results obtained by TEM analyses. The particle sizes of iron oxide nanoparticles and PHB coated nanoparticles visualized by TEM were in the range of 18–20 nm and 30–35 nm, respectively. The hydrodynamic diameters of PHB coated nanoparticles were obtained as about 100 nm in DLS measurements. The higher value of average size obtained in DLS (compared to TEM) originates from the fact that DLS measures the hydrodynamic radii of the particles, which include the solvent layer at the interface. DLS measurements are expected to give the hydrodynamic radius rather than the actual size of the nanoparticles. Therefore, a measurement of the hydrodynamic radius of the nanoparticles would account for the larger DLS measurement than the TEM images because the PHB is expected to have a much smaller configuration when dried on the TEM grid versus in water. This size discrepancy has been observed by others.[31]

TGA

The amount PHB in nanoparticles was measured by thermogravimetric analyzer. The TGA analysis of bare and PHB coated Fe_3O_4 nanoparticles provide qualitative and quantitative information about the volatile components. The TGA curve in Figure 4 shows that the weight loss of bare MNPs over the temperature range from 30 to 850°C is about 3%. This might be due to the loss of residual water in the sample. The PHB-MNPs gave their distinctive TGA curves, which can provide indications of the content of PHB polymer. In Figure 4, at 280°C there is a sharp decrease indicating the combustion of carbon found in PHB. From the result, it can be concluded that the percentage of PHB was around 80% and the amount of magnetite was around 20 wt%. TGA analysis was performed for PHB nanoparticles incubated in PBS for two month and results show similar trends with fresh prepared nanoparticles. Accordingly, polymer loss was not observed for nanoparticles incubated in PBS (pH: 7.2)(data not shown).

VSM

Magnetic hysteresis curve was obtained by VSM. The applied magnetic field was changed and magnetization properties of synthesized Fe_3O_4 and PHB coated Fe_3O_4 nanoparticles were measured at 37°C. Remanence and coercivity were not observed in the hysteresis curve. This phenomenon proved that all nanoparticles synthesized in this study are superparamagnetic. The saturated magnetization (M_S) of bare MNPs is 60 emu/g. The saturated magnetization values were obtained for PHB-MNPs (37 emu/g; Figure 5). Magnetic properties of PHB coated nanoparticles were analyzed with VSM. They were found to be superparamagnetic, which is an essential property for MNPs used for drug delivery systems. Small size is necessary for superparamagnetism and also required to avoid agglomeration of MNPs after applied magnetic field is removed. Magnetic agglomeration can result in blockage of vessels. Therefore, remanence (remaining magnetization) of nanoparticles should be low values and even zero for best. Our VSM analysis showed that PHB coated MNPs are superparamagnetic and have 3–4 emu/g remanence after magnetic field has been removed means magnetization disappears, so there is no risk for blockage of capillary vessels.[32]

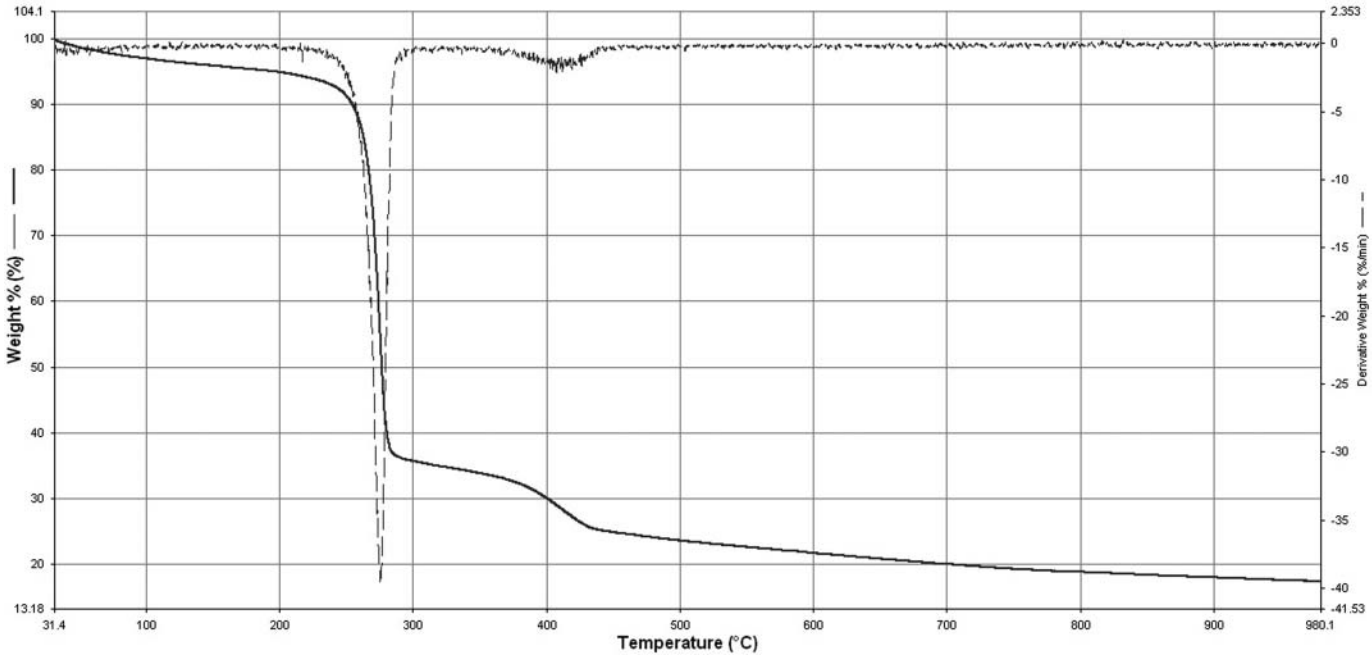

Fig. 4. Thermogravimetric analysis (TGA) of PHB coated iron oxide nanoparticles.

Cellular internalization of PHB Coated MNPs

Endocytosis is known as the main mechanism of cellular internalization for the magnetic nanoparticle vectors.[15] In Figure 6b it is demonstrated by confocal microscopy that most of the PHB-MNPs are taken up by MCF-7 cells. The results are promising due to the fact that, nanoparticles can be internalized into the cells even if they are applied at low concentrations (6.25 μg/mL). Cellular internalization was carried out with five different concentrations (6.25, 12.5, 25, 50, and 100 μg/mL) of PHB coated nanoparticles and a control group. Cell viability was not affected.[33,34] MCF-7,

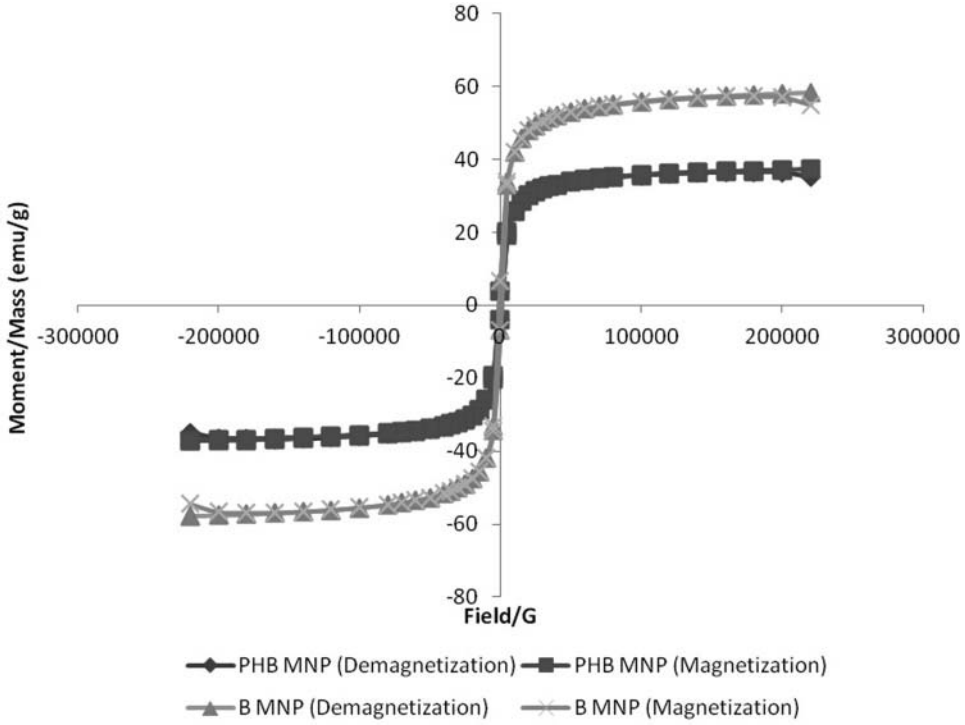

Fig. 5. Vibrating Sample Magnetometer (VSM) results show magnetization curve of the MNPs (60 emu/g) and PHB coated MNPs (37 emu/g) at 37°C.

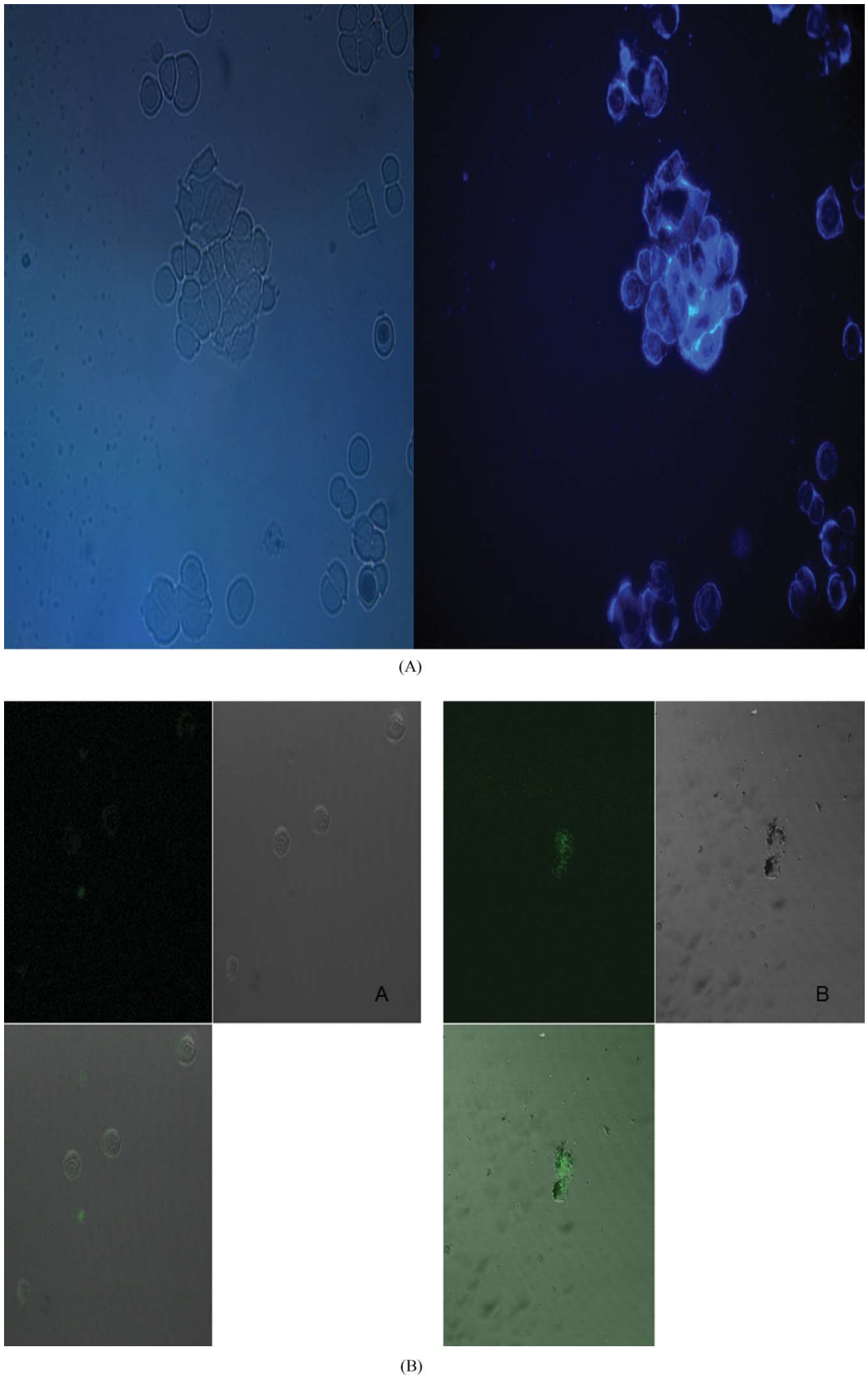

Fig. 6. (a) Image of control MCF-7 breast cancer cells by fluorescence microscopy (20×). **(b)** Cellular internalization of FITC binding PHB-coated MNPs on MCF-7 cells by confocal microscopy (20×; A: control cells, B: treated PHB-MNPs cells). **(c)** Images of cellular internalization of PHB coated MNPs on SKBR-3 cells by fluorescence microscopy (20; cells were stained with FITC dye).

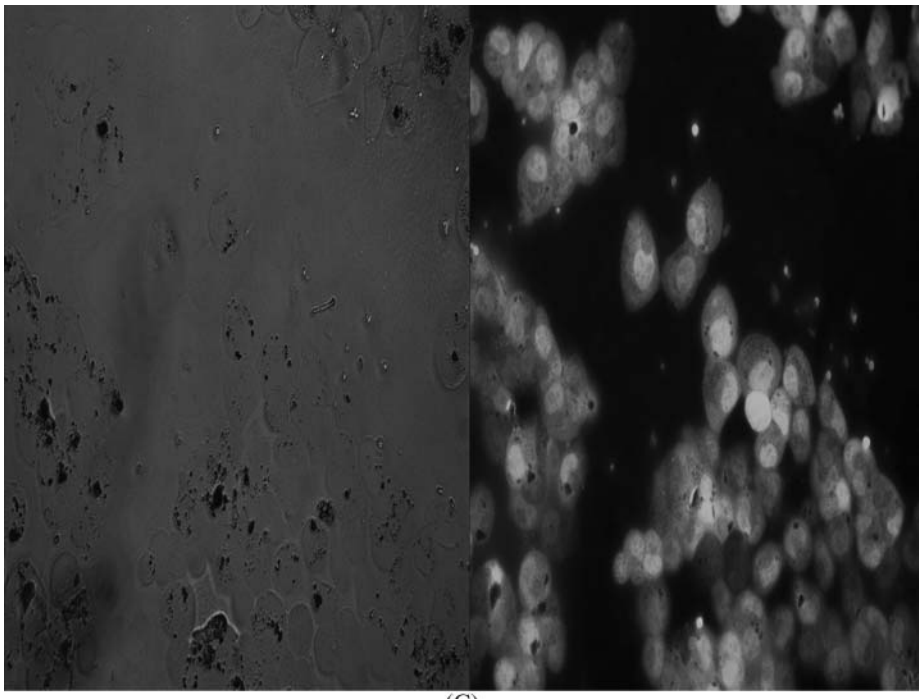

(C)

Fig. 6. (**Continued**).

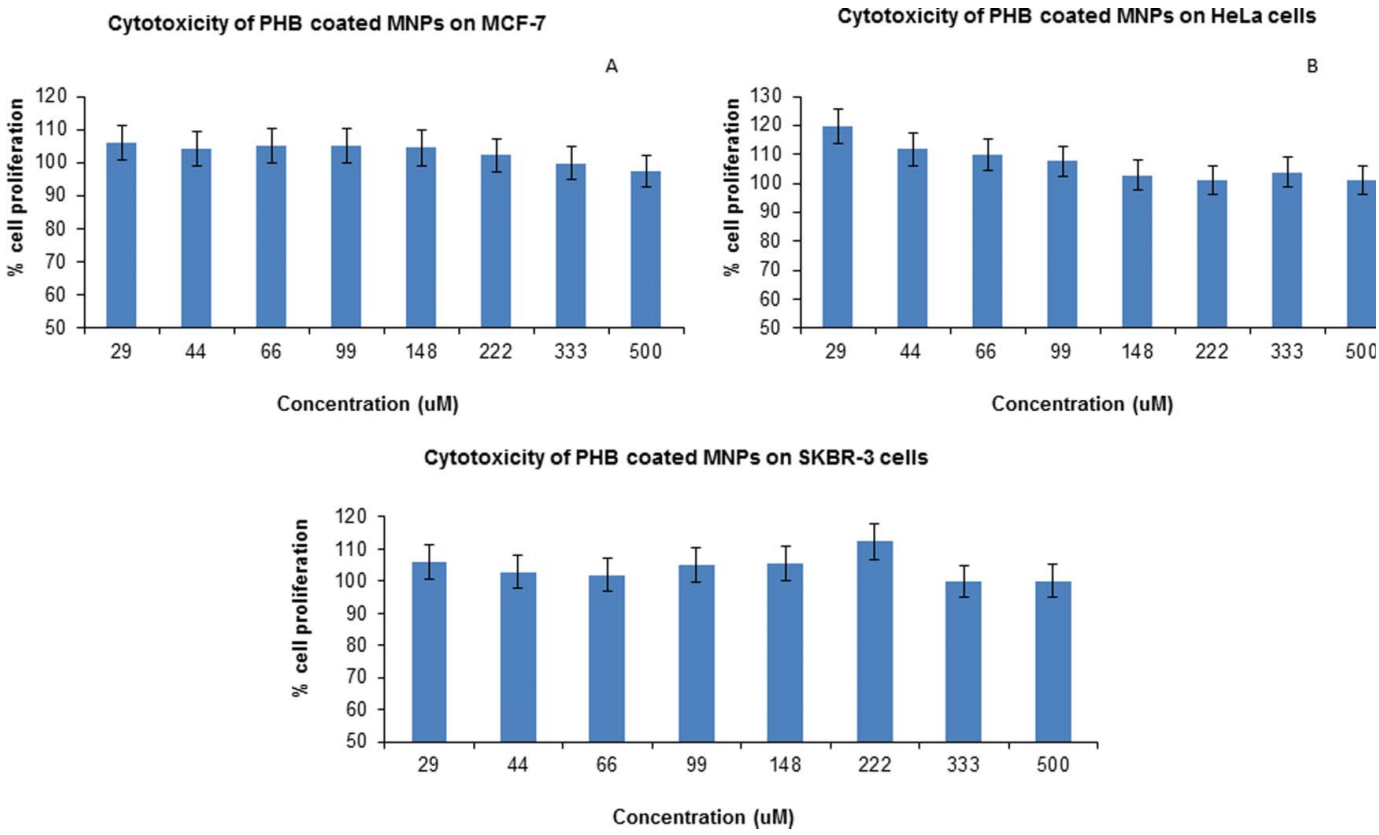

Fig. 7. Cytotoxicity analyses of PHB coated nanoparticles on MCF-7, HeLa, SKBR-3 cells.

SKBR-3, and HeLa cells were treated PHB-MNPs. The internalized PHB coated iron oxide nanoparticles can be observed within the intact cells when compared to control cells (Figure 6a), which were not exposed to nanoparticles. Black dots show the nanoparticles inside the cells.

In Figure 6c it is demonstrated by florescence microscopy that most of the PHB-MNPs are taken up by SKBR-3 cells.

Bare iron oxide nanoparticles were not taken up by the cells due to their negative surface charge coming from the abundant OH- ions (data not shown). After MNPs were modified with PHB, the positive charge increases. Positively charged PHB-MNPs will be easily attached to negatively charged cell membrane, which will result in an increased rate of cellular internalization.[35]

XTT Assay-PHB Coated Nanoparticles Effect on Cell Proliferation

Cytotoxicity of PHB-MNPs was investigated by XTT cell proliferation assay. Survival rates indicated that there is no cytotoxic effect of the nanoparticles. Cells grown in the same medium without any nanoparticle addition was the control group. Their proliferation was taken as 100% (Figure 7). The results of toxicity assay showed that introduction of PHB coated iron oxide nanoparticles did not affect the cell growth. Cells showed excellent growth even in the highest dose of nanoparticles. In the literature, it has been shown that PHB has no cytotoxicity because it is a natural biopolymer and it can be degraded by enzymes in the body. In addition, growth stimulation of PHB nanoparticles was observed both in our study and in the literature.[36]

Comet Assay-PHB Coated Nanoparticles Effect on DNA Damage

Genotoxicity of PHB-MNPs was investigated by Comet assay. The tail DNA contents of PHB coated MNPs treated cells when compared with untreated cells were not detected statistically significant difference ($p < 0.05$). The results of comet assay demonstrated that PHB coated MNPs have not shown genotoxic potential.

Conclusion

This study demonstrated that iron oxide nanoparticles were synthesized and coated with PHB by *in situ* coprecipitation method. The future perspectives of this work would be anti-cancer agent loading to these MNPs, and performing drug release, stability, and cytotoxicity studies in both *in vitro* and *in vivo* systems.

References

1. Wickline, S. A.; Neubauer, A. M.; Winter, P. M.; Caruthers, S. D.; Lanza, G. M. *J. Magnet. Reson. Imag.* **2007**, *25*, 667–680.
2. Corot, C.; Petry, K. G.; Trivedi, R.; Saleh, A.; Jonkmanns, C.; Le Bas, J. F.; Blezer, E.; Rausch, M.; Brochet, B.; Foster-Gareau, P.; Baleriaux, D.; Gaillard, S.; Dousset, V. *Investigat. Radiol.* **2004**, *39*, 619–625.
3. Ferrari, M. *Nat. Rev. Cancer* **2005**, *5*, 161–71.
4. Radad, K.; Al-Shraim, M.; Moldzio, R.; Rausch, W. D. *Environ. Toxicol. Pharmacol.* **2012**, *34*, 661–672.
5. Cattaneo, A. G.; Gornati, R.; Sabbioni, E.; Chiriva-Internati, M.; Cobos, E.; Jenkins, M. R.; Bernardini, G. *J. Appl. Toxicol.* **2010**, *30*, 730–744.
6. Dobson, J. *Gene Therapy* **2006**, *13*, 283–287.
7. Fang, C.; Zhang, M. *J. Mater. Chem*. **2009**, *1*, 6258–6266.
8. McBain, S. C.; Yiu, H. H.; Dobson, J. *Int. J. Nanomed.* **2008**, *3*, 169–180.
9. Polyak, B.; Friedman, G. *Expert Opin. Drug Deliv*. **2009**, *6*, 53–70.
10. Wang, H.; Chen, X. *Expert Opin. Drug. Deliv*. **2009**, *6*, 745–768.
11. Tapan, K. J. *Mol. Pharm.* **2007**, *5*, 316–327.
12. Gao, X.; Chen, J. C.; Wu, Q.; Chen, G. Q. *Curr. Opin. Biotechnol.* **2011**, *22*, 768–774.
13. Verlinden, R. A. J.; Hill, D. J.; Kenward, M. A.; Williams, C. D.; Radecka, I. *J. Appl. Microbiol.* **2007**, *102*, 1437–1449.
14. Unsoy, G.; Yalcın, S.; Khodadust, R.; Gunduz, G.; Gunduz, U. *J. Nanopart. Res.* **2012**, *14*, 964.
15. Lu, A. H.; Salabas, E. L.; Schüth, F. *Angew. Chem. Int. Ed. Engl.* **2007**, *46*, 1222–1244.
16. Vandamme, P.; Coenye, T. *Int. J. Syst. Evol. Microbiol.* **2004**, *54*, 2285–2289.
17. Bonartsev, A. P.; Myshkina, V. L.; Nikolaeva, D. A.; Furina, E. K.; Makhina, T. A. *Appl. Microbiol.* **2007**, 295–307.
18. Jendrossek, D.; Handrick, R. *Annu. Rev. Microbiol.* **2002**, *56*, 403–432.
19. Volova, T. G.; Shishatskaya, E. I.; Sevastianov, V. I.; Efremov, S.; Mogilnaya, O. *Biochem. Eng. J.* **2003**, *16*, 125–133.
20. Zinn, M.; Witholt, B.; Egli, T. *Adv. Drug Deliv. Rev.* **2001**, *53*, 5–21.
21. Tokiwa, Y.; Calabia, B. P. *Biotechnol. Lett.* **2004**, *26*, 1181–1189.
22. Shishatskaya, E. I.; Voinova, O. N.; Goreva, A. V.; Mogilnaya, O. A.; Volova, T. G. *J. Mater. Sci. Mater. Med.* **2008**, *19*, 2493–2502.
23. Clark, P. I.; Slevin, M. L. *Clin. Pharmacokinet.* **1987**, *12*, 223–252.
24. Gewirtz, D. A. *Biochem. Pharmacol.*. **1999**, *57*, 727–741.
25. Xiong, Y. C.; Yao, Y. C.; Zhan, X. Y.; Chen, G. Q. *J. Biomater. Sci. Polym. Ed.* **2010**, *21*, 127–140.
26. Singh, N. P.; McCoy, M. T.; Tice, R. R.; Schneider, E. L. *Exp. Cell Res.* **1988**, *175*, 184–191.
27. Tice, R. R.; Agurell, E.; Anderson, D.; Burlinson, B.; Hartmann, A.; Kobayashi, H.; Miyamae, Y.; Rojas, E.; Ryu, J. C.; Sasaki, Y. F. *Environ. Mol. Mutagen.* **2000**, *35*, 206–221.
28. Merten, C.; Kowalik, T.; Aßhoff, S. J.; Hartwig, A. *Macromol Chem. Phys.* **2010**, 211, 1627–1631.
29. Moghimi, S. M.; Hunter, A. C.; Murray, J. C. *Pharmacol. Rev.* **2001**, 53, 283–318.
30. Yin, Q. Q.; Wu, L.; Gou, M. L.; Qian, Z. Y.; Zhang, W. S.; Liu, J. *Acta Anaesthesiol. Scand.* **2009**, *53*, 1207–1213.
31. Rahman, O.; Mohapatra, S. C.; Ahmad, S. *Mater. Chem. Phys.* **2012**, *132*, 196–202.
32. Arruebo, M.; Pachecco, R. F.; Ibarra, M. R.; Santamaría, J. *Nano-today* **2007**, *2*, 22–32.
33. Wuang, S. C.; Neoh, K. G.; Kang, E. T.; Pack, D. W.; Leckband, D. E. *J. Mater. Chem.* **2007**, *17*, 3354–3362.
34. Mahmoudi, M.; Simchi, A.; Milani, A. S.; Stroeve, P. *J. Colloid Interface Sci.* **2009**, *336*, 510–518.
35. Khodadust, R.; Unsoy, G.; Yalcın, S.; Gunduz, G.; Gunduz, U. *J. Nanopart. Res.* **2013**, *15*, 1488.
36. Chen, C.; Cheng, Y. C.; Yu, C. H.; Chan, S. W.; Cheung, M. K.; Yu, P. H. *J. Biomed Mater. Res. Part A* **2008**, *87*, 290–298.